Available online at www.sciencedirect.com
ScienceDirect
Journal of the European Ceramic Society 28 (2008) 793–801
www.elsevier.com/locate/jeurceramsoc

Thermomechanical modelling of ion-conducting membrane for oxygen separation

E. Blond [a,*], N. Richet [b]

[a] *LMSP (UMR 8106 CNRS/Université d'Orléans/ENSAM Paris), ERT «Design of Ceramic Structures at High Temperature» Polytech'Orléans, 8 rue L. de Vinci, 45072 Orléans, France*
[b] *Air Liquide CRCD, 1 chemin Porte des Loges BP126, 78354 Jouy en Josas, France*

Received 26 May 2007; received in revised form 19 July 2007; accepted 27 July 2007
Available online 24 October 2007

Abstract

Dense mixed ionic conducting membranes are subjected to stresses induced by the oxygen activity gradient under operating conditions. This works proposed a thermomechanical model, taking into account such chemical induced strain. This model permits predictive simulation by the finite element method in transient and steady state to give guidelines for reactor operating conditions optimization. Modelling has shown that the maximum stress on the membrane depends on thermal gradient along the membrane and transient phase's management.

Keywords: Chemical expansion; Ionic conductivity; Perovskites; Membranes; Thermal expansion; Mechanical properties

1. Introduction

Mixed ionic oxygen ceramic membranes are of great interest for applications in catalytic reactors for oxygen separation and conversion of hydrocarbons to value-added products, particularly the conversion of methane to syngas.[1] These materials are exposed to high temperature and oxygen partial pressure gradients.[2] Oxygen vacancies concentration gradient in the material leads to crystal lattice expansion mismatch commonly call chemical expansion.[3,4] Such differences in expansion behaviour could lead to the destruction of the membrane. The understanding and the control of chemical expansion behaviour is of great importance for obvious reliability and safety reasons. A model allowing various thermal and chemical loading was developed in order to obtain guidelines for transient phase management of the reactor.

During the last 10 years a lot of work has been published on chemical induced stresses. Hendriksen et al.[5] prospected especially the syngas production using mixed-conducting ceramic membranes. They considered a tubular membrane under isothermal condition and constant oxygen vacancy gradient. Their work underlines the mechanical benefits of slow reaction kinetics at the membrane surface. Atkinson and Ramos[3] have developed an analytical study of chemical induced stress in planar and cylindrical membranes (biaxial stress) under various mechanical boundary conditions (free, fully constrain, etc.). They assumed that the chemical strain gradient in the depth of the membrane is linear and don't take into account the thermal gradient. This work is a good qualitative comparison between planar and tubular designs under steady state as the assumption of linear chemical expansion gradient is not accurate. Krishnamurthy and Sheldon[2] have developed a thermomechanical model coupled with oxygen vacancies effects writing in the framework of irreversible thermodynamics applied to a SOFC membrane. Unfortunately this model is based on equibiaxial plane stress state with no thermal gradient. They also studied the effect of surface exchange kinetics on stresses and obtained similar results to thermal shock study[6–8]: slow surface exchange rate compare to bulk conductivity is preferred from a mechanical point of view but is not good in term of oxygen permeation. Thermal gradient is not considered, and the authors conclude that the steady state stage is more damaging than transient one.

Analytic models can describe chemical and physical phenomenon but are not easily transposed to complex geometry or loading. Finite element modelling is more appropriate for complex geometry and loading. Yakabe et al.[9,10] have developed

* Corresponding author. Tel.: +33 2 38 49 43 58; fax: +33 2 38 41 73 29.
E-mail address: eric.blond@univ-orleans.fr (E. Blond).

0955-2219/$ – see front matter © 2007 Elsevier Ltd. All rights reserved.
doi:10.1016/j.jeurceramsoc.2007.07.024

a finite element model taking into account chemical expansion based on the correlation between the oxygen vacancies concentration in the material and the relative expansion. Vacancies distribution is converted to an equivalent thermal field – simulating the induced strain – and used in mechanical calculation. This method is applied to SOFC membranes under steady state and under stepwise change of atmosphere. The calculation of an equivalent thermal gradient to simulate chemical expansion does not allow fully transient and coupled simulation as temperature and oxygen vacancy are included within one variable. The goal of this work is to build a model allowing fully coupled and transient computation in order to test various geometries and/or loadings. This paper will focus on loadings concerns.

The model developed in this work divides the strain into three independent parts: elastic strain, thermal strain and chemical strain. Chemical strain is directly related to the oxygen concentration in the material (or equivalent oxygen activity) which is one of the state variables of the model. All the calculations are realized with the same finite element code in which Wagner's law and chemical expansion behaviour have been implemented. Simulation of coupled permeation and temperature under transient conditions were carried out. The effects of material properties and operating conditions, especially atmospheres variation rates, on stresses in the membrane were evidenced using this model.

After a brief description of the material expansion behaviour under various atmospheres, the identification of the model of chemical expansion using experimental results is exposed. Then, the implementation of the expansion model in the finite element code ABAQUS is shortly explains and the strategy adopted to run simulation is presented. Finally, the impact of operating conditions on stress distribution and its evolution in the membrane are discussed.

2. Experimental and expansion behaviour

Many works have established the relation between chemical-induced expansion of electrochemical ceramic and oxygen partial pressure mismatch between manufacturing and operating conditions.[5,11–14] The material used in this study is made of lanthanum, strontium, titanium and iron ($La_{0.495}Sr_{0.396}Fe_{0.9}Ti_{0.1}O_{3-\delta}$) and exhibit a perovskite structure. It has been sintered under inert atmosphere (N_2) at 1250 °C for 2 h. The expansion behaviour has been measured on a NETSCH 402ED dilatometer using bars of 5 mm × 5 mm × 8 mm. Atmospheres were adjusted using two mass flow controllers, one for pure oxygen and one for pure nitrogen.

The expansion behaviour has been measured under various oxygen partial pressures under linear increase of temperature using a 2 °C/min heating rate and under isothermal conditions. For isothermal tests, the heating was carried out under nitrogen at 2 °C/min and the atmosphere was modified after the stabilization of the dwell temperature. Isothermal expansion is recorded for 2 h and the cooling is carried out under the same atmosphere.

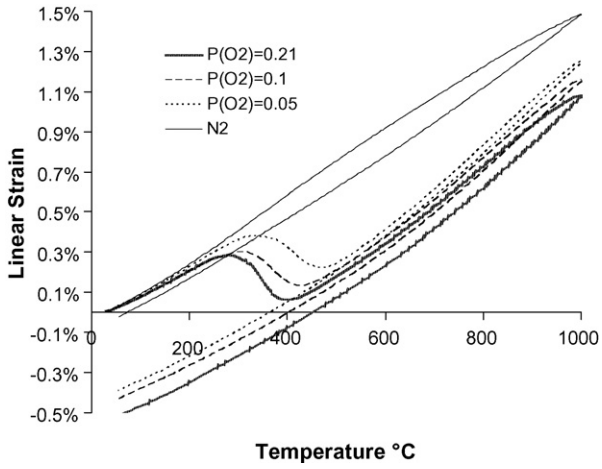

Fig. 1. Linear increase of temperature expansion behaviour under various oxygen partial pressure of LSFT material sintered under N_2.

Fig. 1 presents the expansion behaviour of the material under linear increase of temperature and various oxygen partial pressures. The curves under oxidizing atmospheres show three stages. Before 300 °C, the expansion is purely thermal. Between 300 °C and around 450 °C a contraction is recorded due to oxygen uptake inducing crystal lattice parameter decrease until the material reaches thermodynamic equilibrium. Above this temperature, the expansion is probably the sum of pure thermal expansion and chemical expansion due to vacancy creation and annihilation in equilibrium with temperature and oxygen partial pressure. As no chemical expansion is observed during cooling, we can conclude that the material is fully stabilized. A test under N_2 confirms that under the same atmosphere as the sintering one the material is stable. The hysteresis recorded under inert atmosphere can be associated to sintering and/or small oxygen activity difference between sintering and expansion measurement atmospheres.

The beginning of chemical-induced contraction seems to be oxygen partial pressure dependant. This difference could be due to surface effects as activation depends on temperature but also on surface exchange kinetic. The thermal activation of the bulk oxygen diffusion seems to be independent on oxygen partial

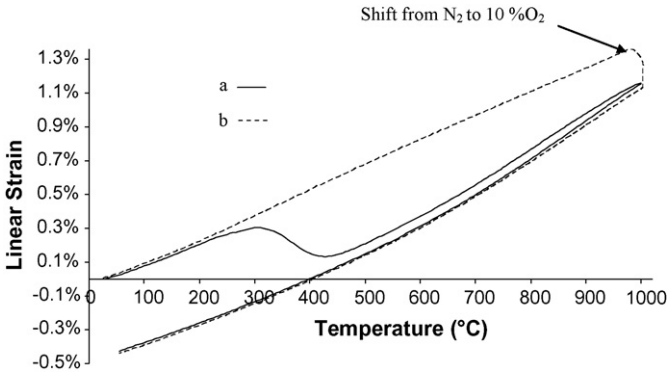

Fig. 2. Comparison of (a) expansion behaviour under linear increase of temperature under 10% of oxygen and (b) isothermal expansion at 1000 °C from N_2 to 10% of oxygen.

pressure. However, the total oxygen flux through the membrane depends strongly on the oxygen partial pressure gradient.[14]

Fig. 2 shows on the same graph the expansion behaviour under linear increase of temperature under 10% of oxygen and the isothermal expansion behaviour at 1000 °C for 2 h under 10% of oxygen as describe above. Below 300 °C, the strain slopes are similar for both linear increases of temperature and isothermal tests while permeation is not activated. During cooling the curves are superimposed indicating that the material is fully stabilized after both tests. As the only difference between those tests is the atmosphere during heating these results clearly show that final chemical induced strain is independent of the temperature. The final residual chemical strain depends only on the oxygen partial pressure in the material (i.e., oxygen activity) as thermal strain depends only on temperature. This observation leads to the development of a thermomechanical model with strain partition hypothesis adding the oxygen partial pressure as state variable for chemical expansion.

3. Constitutive equations of the thermomechanical behaviour

The material is assumed to be homogeneous, isotropic, and to have linear thermo-elastic behaviour. Chemical induced strain does not modify this behaviour but comes in addition to the usual thermal expansion.[11] In this work we used a relation between macroscopic expansion behaviour and chemically or thermally induced strain. This relation is written according to the classical mechanical way, using the strain partition hypothesis and a phenomenological point of view.

Let $\boldsymbol{\varepsilon}$ be the total strain tensor. Assuming small strains, the total strain tensor is described by the symmetric part of the gradient of the displacement vector $\mathbf{u} = \mathbf{u}(\mathbf{X})$ with respect to the spatial position $\mathbf{X}$ in the material:

$$\boldsymbol{\varepsilon} = \frac{1}{2}\left(\frac{\partial \mathbf{u}}{\partial \mathbf{X}} + \left(\frac{\partial \mathbf{u}}{\partial \mathbf{X}}\right)^{\mathrm{T}}\right) \tag{1}$$

Moreover, the total strain can be expressed as follows.

$$\boldsymbol{\varepsilon} = \boldsymbol{\varepsilon}_{\mathrm{t}} + \boldsymbol{\varepsilon}_{\mathrm{e}} + \boldsymbol{\varepsilon}_{\mathrm{c}} \tag{2}$$

where $\boldsymbol{\varepsilon}_{\mathrm{t}}$ is the thermal strain tensor, $\boldsymbol{\varepsilon}_{\mathrm{e}}$ the elastic strain tensor and $\boldsymbol{\varepsilon}_{\mathrm{c}}$ is the chemical strain tensor, respectively. In the rest of this paper, bold symbol will refer to vector/tensor variable and normal ones will refer to scalar parameters.

The behaviour of the material is assumed to remain isotropic with similar properties in tension and in compression. It is commonly accepted that ceramics follow this assumption but more complex mechanical behaviour can easily be used.[15]

The thermal strain tensor depends only on temperature variation in a reversible way:

$$\boldsymbol{\varepsilon}_{\mathrm{th}} = \alpha(T - T_0)\mathbf{I} \tag{3}$$

where α is the secant coefficient of linear thermal expansion, T_0 a reference temperature and $\mathbf{I}$ the second rank identity tensor. The coefficients of thermal expansion (α) of our material are presented in Table 1.

Table 1
Coefficient of thermal expansion of LSFT material

Temperature (°C)	α ($\times 10^{-5}$) (/°)
175	1.3
400	1.6

The elastic strain tensor depends only on stress variation in a reversible way:

$$\boldsymbol{\varepsilon}_{\mathrm{e}} = \frac{1+\nu}{E}\boldsymbol{\sigma} - \frac{\nu}{E}\mathrm{Tr}(\boldsymbol{\sigma})\mathbf{I} \tag{4}$$

where ν is the Poisson ratio, E the Young modulus and $\boldsymbol{\sigma}$ is the stress tensor.

The main assumption of our model is the reversible dependence of the chemical strain tensor with oxygen partial pressure variation.[16] The identification of this dependence has been carried out using expansion tests. The curves obtained show a residual deformation at the end of the test (see Figs. 1 and 2). Assuming that the time spent above the temperature of activation for the oxygen diffusion is long enough, the oxygen partial pressure, in sense of activity, in the material at the end of the test will be the same as in the atmosphere of test. The total chemical expansion is constant in this range of temperature whatever the oxygen partial pressure. So, for any temperature above oxygen diffusion activation zone:

$$\varepsilon_{\mathrm{go}} - \varepsilon_{\mathrm{back}} = (\varepsilon_{\mathrm{e}} + \varepsilon_{\mathrm{t}}) - (\varepsilon_{\mathrm{e}} + \varepsilon_{\mathrm{t}} + \varepsilon_{\mathrm{c}}) = -\varepsilon_{\mathrm{c}} \tag{5}$$

where ε refers to linear strain in the direction of expansion measurement. The identification of the linear chemical strain obtained using Eq. (5) is summarized in Fig. 3. It is important to note that specimens subjected to isothermal expansion under various oxygen partial pressure, between 15% and 21% of oxygen, exhibit cracks observed with an optical microscope.

In a first approach, two linear extrapolations fit the experimental results in Fig. 3. Only three parameters are necessary to describe such model:

- P_{r}, the partial pressure of slope modification (0.05)

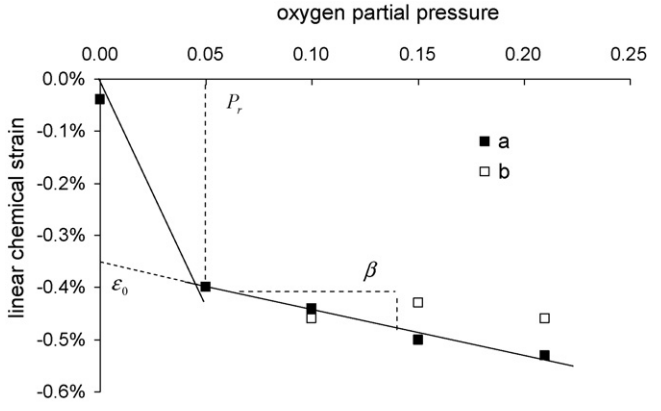

Fig. 3. Chemical strain vs. oxygen partial pressure: (a) results from linear thermal expansion tests and (b) results from isothermal expansion tests.

- β, the chemical strain slope for partial pressure higher than P_r (0.0082)
- ε_0, the instantaneous chemical strain (0.0037)

As strain and partial pressure are dimensionless those parameters also have no dimension. Assuming that the chemical strain is isotropic, as thermal expansion, its dependence versus oxygen partial pressure can be described by the following equations:

$$\begin{cases} P \geq P_r & \boldsymbol{\varepsilon}_c = -(\beta P + \varepsilon_0)\mathbf{I} \\ P \leq P_r & \boldsymbol{\varepsilon}_c = aP\mathbf{I} \end{cases} \quad (6)$$

with

$$a = -\beta - \frac{\varepsilon_0}{P_r} \quad (7)$$

The instantaneous strain ε_0 can be defined as character "chemical shock" due to fast variation of oxygen partial pressure. At low oxygen partial pressure the instantaneous deformation is a critical phenomenon. It is in accordance with the idea of two different mechanisms at low and high oxygen partial pressure,[17] i.e. oxygen vacancy at low P_{O_2} and oxygen interstitial at high P_{O_2}. But it needs further investigation to be certain of the origin of the initial strain gap. However, the critical oxygen partial pressure, at which the transition between those two mechanisms occurs may be lower than 0.05. Above this value, the linear dependence of the chemical strain with oxygen partial pressure seems to be a good approximation. A logarithmic relation between chemical strain and partial pressure would also fit well the experimental results in the all range of oxygen partial pressure. More experiments at very low oxygen partial pressure are necessary to determine the proper model. However, trend remains the same.

The transition between sintering atmosphere and very low oxygen partial pressure is a critical point in term of strain management. Very fast deformation of the material occurs in this range of oxygen partial pressure. This phenomenon is similar to thermal shock. Above a critical oxygen partial pressure (P_r), the dependency of the chemical induced strain with oxygen partial pressure variation is smaller. The ability of the material to resist fast oxygen partial pressure variation can be evaluated using the slope β that is the linear tangential chemical expansion coefficient for high oxygen partial pressure.

These parameters are guidelines to warranty the integrity of the membrane during transient phases. Furthermore, very high values of ε_0 or very low values for P_r may lead to a systematic destruction of the membrane at the start up of the reactor. As shown hereafter, these parameters and material Young modulus (and Poisson ratio) permit a quick estimation of chemical induced stresses.

4. Computation method

The mechanical behaviour described above has been implemented in ABAQUS[18] finite elements software using the UMAT[18] procedure. Computations are realized in three stages:

1. Heat transfer computation to obtain the temperature field in the bulk of the membrane. This calculation is performed with the finite element code ABAQUS[18] using classical thermal boundary conditions and loading or with dedicated routines taking into account chemical reactions and fluid dynamics in CFD code such as FLUENT.[19]
2. The oxygen partial pressure field in the bulk of the membrane is calculated, using ABAQUS,[18] from the temperature gradient obtained in stage 1 and the initial conditions on oxygen partial pressure as boundary conditions.
3. Thermomechanical simulation including a dedicated material behaviour, the temperature gradient obtained in stage 1 and the oxygen partial pressure distribution obtained in stage 2 is carried out with ABAQUS.[18]

Stage 3 calculations necessitate the definition of a new variable for oxygen partial pressure in ABAQUS. Even if oxygen partial pressure has no physical meaning in a solid, it is used as a state variable so it has to be understood as the chemical activity of oxygen in the material.

Stage 2 requires a macroscopic modelling of oxygen permeation through the membrane. Bulk diffusion and surface exchange mechanisms are in competition.[20] Pure bulk diffusion can be represented using the Wagner law[14]:

$$\mathbf{J} = -\frac{RT}{16F^2}\frac{\sigma_{ion}\,\sigma_{el}}{\sigma_{ion}+\sigma_{el}}\mathrm{grad}(\mathrm{Ln}(P_{O_2})) \quad (8)$$

where $\mathbf{J}$ is the oxygen flux, R the gas constant, F the Faraday constant, σ_{ion} the ionic conductivity and σ_{el} is the electronic conductivity. Electronic and ionic conductivities come from Nernst–Einstein relation as a function of the chemical diffusivity of oxygen D and vacancy concentration C_v. Assuming the ionic conductivity to be much lower than electronic conductivity ($\sigma_{el} \gg \sigma_{ion}$):

$$\mathbf{J} = -\frac{C_v D}{4}\mathrm{grad}(\mathrm{Ln}(P_{O_2})) \quad (9)$$

Oxygen diffusion coefficient and vacancy concentration are temperature dependent and follow an Arrhenius law. In a first approximation we assumed that those parameters do not dependent on the oxygen activity. This assumption is commonly accepted for oxygen diffusion whereas talking about oxygen vacancy concentration; it is only acceptable if it reaches a high level after sintering with small variations in operation. As the model developed herein does not take into account vacancy formation, it is limited to specific material formulations. However, this phenomenon can be taken into account if necessary. The expression of the oxygen flux is the following:

$$\mathbf{J} = D_0 e^{-Q/RT}\frac{\partial \ln P_{O_2}}{\partial \mathbf{X}} = \frac{D_0 e^{-Q/RT}}{P_{O_2}}\frac{\partial P_{O_2}}{\partial \mathbf{X}} \quad (10)$$

where $\mathbf{J}$ is the oxygen flux, D_0 an "oxygen diffusivity" coefficient, Q the activation energy, R the gas constant and P_{O_2} is the oxygen partial pressure. From a numerical point of view, the oxygen partial pressure is similar to temperature and the Wagner's law is similar to heat transfer (or Darcy's law) with non-constant diffusivity. Wagner's law expression has been adapted to use the standard heat transfer procedure, existing in ABAQUS 6.5,[18] to

Table 2
Identified value for oxygen diffusion computation

Partial pressure, P_{O_2}	Activation energy, Q (kJ mol^{-1})	"Intrinsic" diffusivity, D_0 (m^2 s^{-1})
0.21	70.4	
0.10	80.2	1.7×10^{-6}
0.05	95	

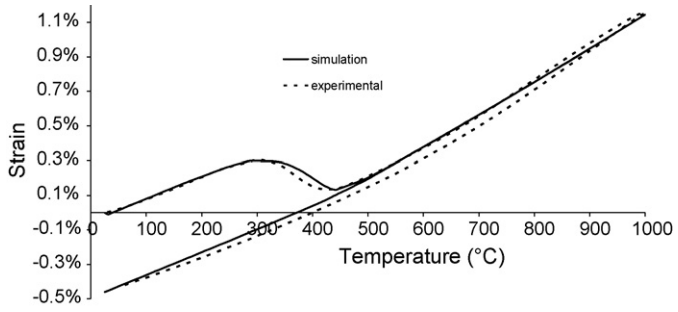

Fig. 4. Identification of the Wagner's law coefficient D_0 and Q (Eq. (10)) for 10% of oxygen partial pressure.

calculate the oxygen gradient in the bulk of the material (transient or steady state). Heat transfer analogy allows the modelling of surface effects using oxygen flux boundary conditions. In this work, as surface effects have been neglected, oxygen partial pressure value at the boundary is the one in the atmosphere.

D_0 and Q values of Eq. (10) presented in Table 2 have been identified on all expansion tests using an inverse method. As heat diffusion is much faster than oxygen diffusion, thermal expansion tests were computed using the heating rate of the test itself and assuming a homogeneous temperature field on the sample. Various oxygen partial pressures were applied on the surface of the specimen. Be aware that the definition of the diffusivity D_0 is not the usual one (see Eq. (10)). As shown in Fig. 1, the temperature of oxygen diffusion mechanism activation depends on the oxygen partial pressure. This relation can be attributed to surface effects related to the initial oxygen partial pressure (activity) mismatch between the surrounding atmosphere and the specimen itself. As surface effects have been neglected, from now, the choice of pressure dependent activation energy has been made to take into account the dependence of the activation temperature with oxygen partial pressure. Vacancy formation may also be involved so that this activation energy is not related to one single mechanism but merge all the mechanisms that govern oxygen diffusion. As shown in Fig. 4, such macroscopic approach is consistent with experimental data.

5. Thermomechanical simulations of an oxygen separation unit

Permeation experiments have been realized on tubular membranes of 252 mm length, 7.2 mm inside diameter and 1 mm thickness. The membrane is submitted to a high thermal gradient as the sealing with the reactor must be maintained at low temperature (Fig. 5).

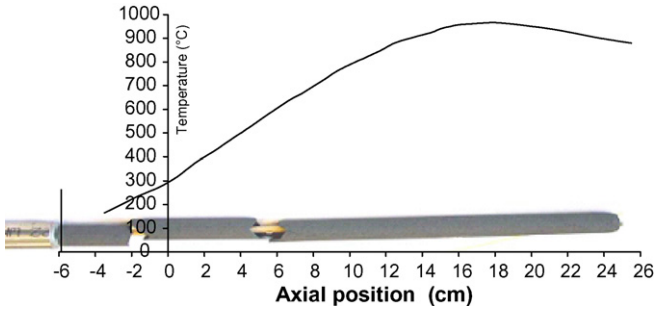

Fig. 5. Permeation test and failures position.

The test procedure is the following. First of all, the membrane is heated under inert atmosphere. Second, after reaching a thermal steady state, the oxygen partial pressure is modified in the inside of the tube from N_2 to 21 % of O_2. Third, various oxygen partial pressure gradients are applied through the membrane by maintaining the inert atmosphere or by introducing a reducing atmosphere on the outside of the tube. Using this procedure, cracks are systematically observed at the same distance from the sealing (Fig. 5): 5.6 cm and 11.2 cm. According to the thermal gradient along the membrane cracking occurs around 260 °C and 530 °C.

Sealing has been modelled in the thermo mechanical simulation using boundary conditions. Axial displacements at the bottom of the tube are restrained and radial displacements are free. It corresponds to a tube supported by a metal ring with a radial sealing infinitely flexible. In the same way, the joint between the reducing atmosphere and the external atmosphere is assumed to be infinitely flexible, so it has not been model by mechanical boundary conditions (see Fig. 6).

The tubular membrane has been modelled in 2D with eight nodes axisymmetric elements. The same meshes have been used for each stage to avoid numerical interpolation between calculation steps. In the same manner, to avoid time interpolation between each computation, the time increment remains constant for each stage. Temperature gradient measured in the furnace

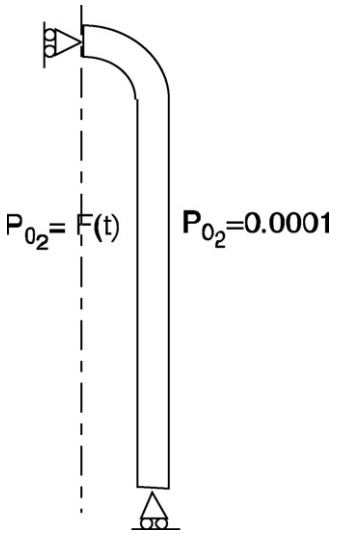

Fig. 6. Boundary conditions used in the model.

Table 3
Physical and mechanical properties of LSFT material

Density, ρ (kg m^{-3})	6200
Young modulus, E (GPa)	30
Poisson's coefficient, ν	0.25
Tensile strength (MPa)	97
Thermal conductivity, λ (W m^{-1} °C^{-1})	2
Specific heat, C_p (J kg^{-1} °C^{-1})	500

using thermocouple at the outside of the membrane has been used for thermal loading and heat transfer computation. The obtained temperature distribution has been used for oxygen diffusion simulation through the membrane.

Table 3 summarizes the properties of the material used for thermo mechanical computation. Young modulus and tensile strength have been measured by four point bending tests on a MTS-2/M testing machine with a load sensor of 10 kN. Ten specimens of 6 mm × 3 mm × 61 mm have been tested for statistical reasons. The Young modulus has been found equal to 30 GPa and the tensile strength is equal to 97 MPa with a Weïbull modulus of 7.7. The Poisson ratio has been chosen equal to 0.25, a standard value for such ceramics. Thermal conductivity and specific heat have been obtained by flash laser method.

Due to the chemical expansion, induced by oxygen permeation, the inside surface of the membrane is in tension and the outside in compression. The highest value of the maximal principal stress (Rankin criterion) is situated on the inside surface of the membrane. Fig. 7 shows the evolution of the maximal stress in the inside of the membrane with time in the case of oxygen partial pressure modification from $P_{O_2} = 0$ to 0.21 in 5 min followed by a dwell of 5 min under $P_{O_2} = 0.21$. The maximal stress level is situated at 11.6 cm from the sealing. This is in good accordance with cracks observed on membrane after permeation tests carried out using the same procedure.

Fig. 7 shows that the stress level is not equal to zero in the first 5 cm. This result is an artefact due to oxygen partial pressure boundary conditions imposed on the surface of the membrane. As the temperature is too low in this zone for oxygen diffusion to occur, no chemical expansion and no stress should be obtained. The model could be improved by using boundary conditions taking into account thermally activated surface effects. Therefore, the stress gradient between 5 cm and 10 cm is underestimated that could explain the crack observed at 5.6 cm from the sealing. As this crack is close to the furnace entrance, the design of this part may also be involved.

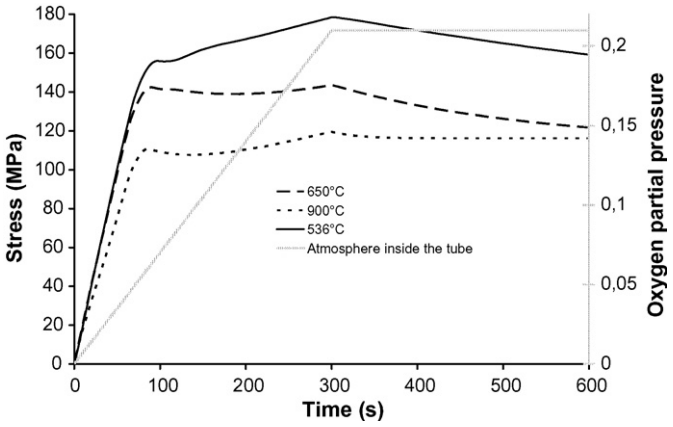

Fig. 8. Evolution of the maximal principal stress with time at different abscissa/temperature.

As shown in Fig. 1 chemical induced expansion takes place in the temperature range of 300 °C to 450 °C depending on oxygen partial pressure. From Figs. 5 and 7 the stress level increases at 400 °C and the maximal stress level is reached around 500 °C. These results are consistent with experimental failure of tubular membrane that occurs at 536 °C. Stress level in the membrane seems to be mainly driven by oxygen diffusion kinetic and temperature gradient along the membrane.

Fig. 8 shows the evolution of the maximal stress with time at three levels of temperature on the inside of the membrane surface. Maximal stress level decreases from 536 °C to 900 °C whereas the rate of stress increase remains the same. Those results can be explained regarding Fig. 9. Oxygen partial pressure gradient in the section of the membrane decreases as temperature increases. The difference is much more important

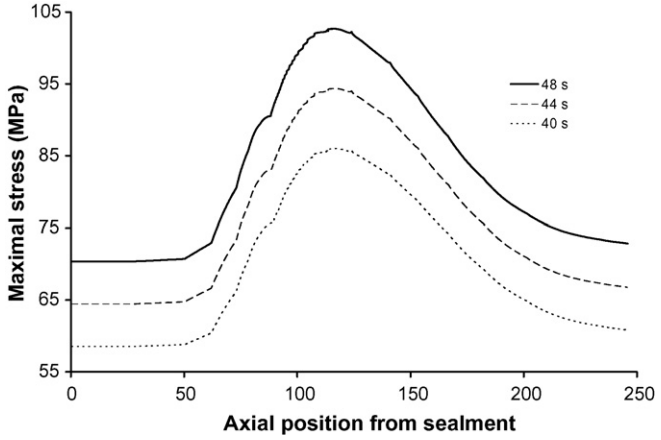

Fig. 7. Maximum principal stress on the inside surface along axis at different time for an oxygen partial pressure modification from 0 to 0.21 in 5 min and a dwell of 5 min under $P_{O_2} = 0.21$.

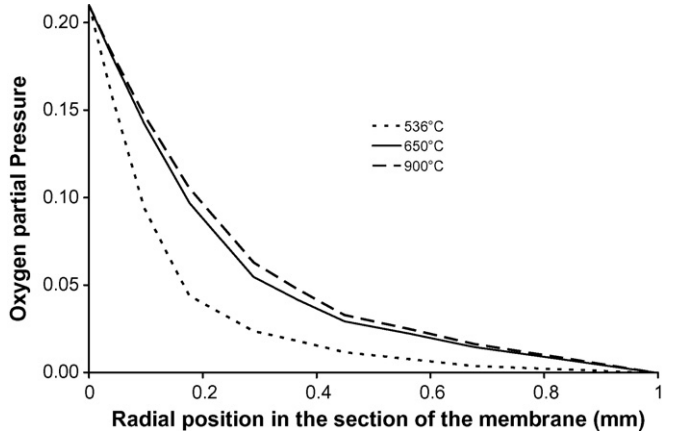

Fig. 9. Oxygen activity profile in the radial section of the membrane after oxygen partial pressure variation from $P_{O_2} = 0$ to 0.21 in 5 min and a dwell of 5 min at $P_{O_2} = 0.21$.

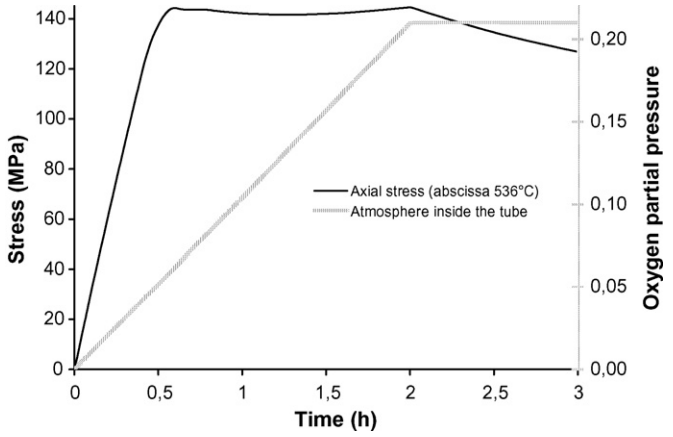

Fig. 10. Evolution of the maximal principal stress with time for slower atmosphere modification rates.

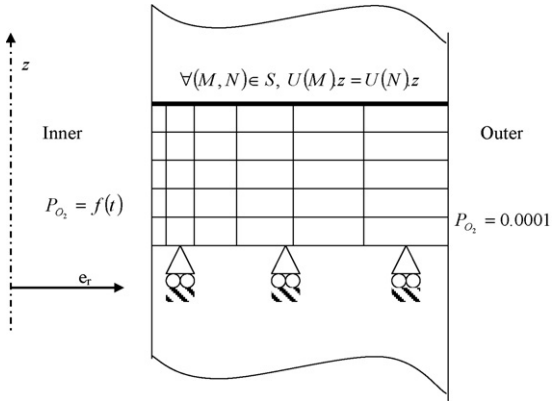

Fig. 11. 2D part of the membrane used for simulation.

between 536 °C and 650 °C than between 650 °C and 900 °C. As oxygen diffusion is thermally activated, the oxygen activity gradient in the section of the membrane decreases with temperature increase. As the stress level is directly linked to oxygen activity gradient in the membrane, high oxygen diffusion rate reduces stresses in the membrane.

Fig. 10 shows the evolution of the maximal principal stress with time for a slower oxygen partial pressure modification rate. Oxygen enrichment between, 0.0001 and 0.21 has been carried out in 2 h. The maximal stress level reached at 536 °C is lower using slow enrichment rate than in the previous case, respectively 144 MPa and 178 MPa.

Figs. 8 and 10 show that the stress level decreases with time under atmosphere and temperature steady state. This phenomenon can be attributed to the decrease of the oxygen activity gradient in the section of the membrane as a steady state of oxygen diffusion takes place. In those two computations, the steady state was not reached, even for 900 °C (Fig. 8). Indeed, after a fast increase of stress level, it decreases very slowly because of the permeation kinetics driven by the partial pressure gradient according to the Wagner law. Similar phenomenon is well known regarding thermoelasticity and the analogy between thermally induced shock and chemically induced shock has been made.

Thermal gradient along the membrane, oxygen partial pressure modification rate and oxygen diffusion kinetic through the membrane have been identified as the key parameters to control stress level in the membrane. From the results obtained using the model described in this work and from a thermo mechanical point of view, the membrane should be operated under isothermal conditions and at the highest temperature to decrease stress level. A parallel has been made between thermal and chemical induced stresses and the concept of chemical shock has been introduced.

6. Atmosphere variation rates effects on stress level

The effects of the atmosphere variation from inert to air has been studied considering the previous tubular membrane under isothermal conditions at 650 °C and modifying the oxygen partial pressure on the inside surface of the membrane. The outside oxygen partial pressure remains constant. Taking into account symmetry considerations, a small part of the membrane will be modelled in 2D (Fig. 11). The bottom and the top surfaces have been constrained to remain flat to take into account the all-tubular membrane. Four nodes axisymmetric elements are used for oxygen diffusion calculation and eight nodes axisymmetric elements for mechanical computations.

It is assumed that the initial oxygen activity in the membrane is equal to 0.0001 as sintering has been carried out under N_2 and that initial partial pressure in the inside and at the outside of the membrane is the same. Several variation rates of the oxygen partial pressure inside the tube were simulated.

Fig. 12 shows the axial stress distribution in the membrane during atmosphere variation, on the inside surface of the membrane (abscissa = 0) from inert atmosphere to air within 70 min. The two different durations (1028 s and 5400 s) are respectively related to the transient state and the steady state. Stress distribution profiles are very different. The transient state is characterized by a higher maximal stress on the inside surface of the membrane, 98.6 MPa instead of 83 MPa after 1 h and 30 min. Even if the tensile stresses are lower during steady state, a larger zone is affected. To ensure momentum balance, the outside surface is subjected to an axial compressive stress greater than 112 MPa. During transient state a small axial compression stress

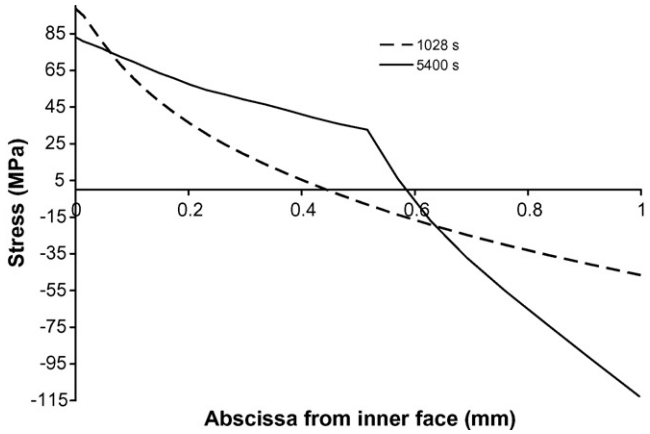

Fig. 12. Evolution of the axial stress during a linear variation of the inside atmosphere from inert to air in 70 min.

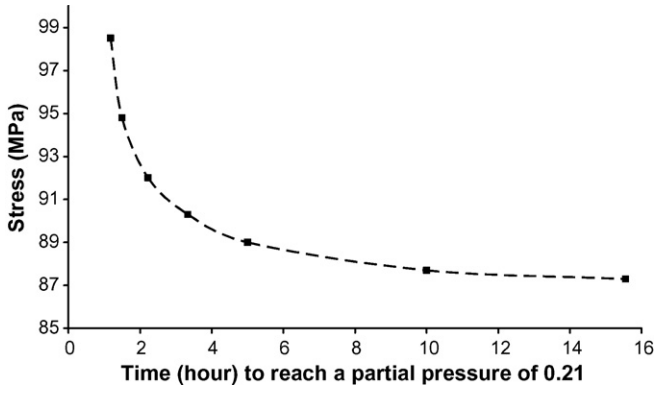

Fig. 13. Maximal transient stress vs. time to change atmosphere from N_2 to air.

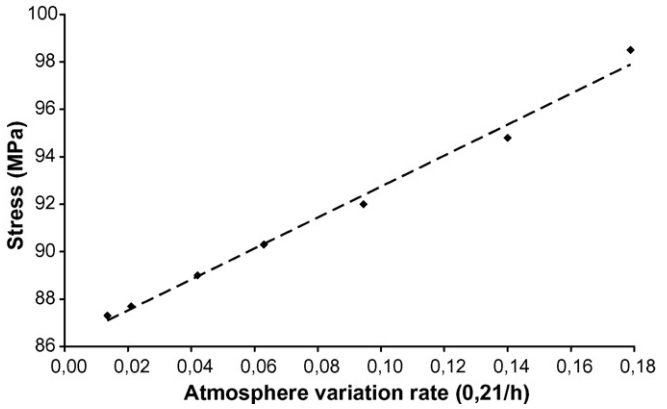

Fig. 14. Maximal transient stress vs. atmosphere variation rate in the inside of the tubular membrane from inert to air.

(46 MPa) is observed and the area under traction is smaller. It is obvious that transient is the most dangerous because of higher tensile stress level, but the axial stress profile during steady state should favour default sensibility because of the volume effect.[21]

Fig. 13 shows the impact of atmosphere variation rate on the maximal stress level in the membrane. At the beginning the curve exhibits a fast decrease with time that becomes much smaller after 5 h. For instantaneous atmosphere variation, the stress level seems to be infinite. However, a numerical estimation of the maximal stress was carried out leading to 500 MPa. This result is not reported in Fig. 13 for results description convenience.

Assuming a linear chemical expansion relation with oxygen partial pressure variation, the dependence of the stress level with atmosphere variation rate can be roughly explained by a simplified analytical approach based on thermal stress analogy. In a first approach chemical strain is expressed by the following equation:

$$\varepsilon_c = \gamma(P - P_0) \tag{11}$$

with γ the linear chemical expansion coefficient, P the current oxygen partial pressure, P_0 the initial oxygen partial pressure.

By analogy with thermal stresses, the analytical solution of a tubular membrane "heated" from the inside, during steady state in generalized plane strain can be expressed by[22]:

$$\sigma(x) = \frac{\gamma E}{2(1-\nu)}(P_m - P(x)) \tag{12}$$

with P_m the average oxygen partial pressure in the section of the membrane. This result is the same for thermal shock. It confirms that chemical shock should be taken into account. Moreover, a part of the thermal shock theory[6–8] can be used. Then, we proposed a little variation of these approaches to obtain guidelines for operating conditions optimization.

Assuming that the average oxygen activity variation in the membrane is very low at the beginning of the oxygen partial pressure modification on the inside of the membrane and that the maximal stress level is located near the inside surface, until a characteristic time τ is reached, the maximal stress is only dependent on the difference between surface and average partial pressure:

$$\sigma_{max} \approx \frac{\gamma E}{2(1-\nu)}(P_m - \dot{P}_1 \tau) \tag{13}$$

with $\dot{P}_1$ the oxygen partial pressure variation rate.

In the case of a non linear relation between chemical expansion and oxygen partial pressure variation, Eq. (13) should be re-write with the value γ on the surface and the appropriate average pressure in the section of the membrane:

$$P_m = \frac{1}{e}\int_0^e \gamma P_{O_2}\, dx \tag{14}$$

In any case, the characteristic time depends mainly on oxygen diffusion rate. So a linear relation should exist between the maximum stress and oxygen partial pressure variation rate.

Fig. 14 shows the evolution of the maximal stress (obtained by numerical simulation) versus oxygen partial pressure variation rates. These results confirm that the operating conditions have a great influence on mechanical stress development during transient phases, and so on the membrane lifetime. From Fig. 14 it is possible to determine the maximal variation rate of the oxygen partial pressure to prevent membrane damages or breakage.

In the specific case of the material consider in this work, its tensile strength (97 MPa) is higher than the steady state tensile stress level (83 MPa). To ensure membrane integrity during start up procedure, it is recommended not to exceed an oxygen partial pressure variation rate above 0.14 h^{-1} (see Fig. 14). Simulation results were confirmed by experimental observations on tubular membranes. Indeed, many successful starting up with different materials have been realized with this recommendation.

7. Conclusion

Assuming oxygen partial pressure as a state variable, and a direct dependence of the chemical induced strain and after the macroscopic and phenomenological modelling of the chemical induced expansion proposed herein; materials can be classified in term of "instantaneous chemical strain", denoted ε_0, and chemical strain slope, denoted β. The first coefficient may be related to "chemical shock", or to fast atmosphere variation in

the low oxygen partial pressure range (below 0.05); the second parameter may be related to the ability of the ceramic to accommodate fast variation of the atmosphere in the high oxygen partial pressure range (above 0.05).

The model of the chemical strain, proposed in this work, include chemical, thermal and mechanical behaviour under transient and steady state conditions. Expansion measurements carried out under various oxygen partial pressures are fitted assuming a Wagner law for oxygen diffusion. However if surface effects become dominant, oxygen diffusion model should be modified by changing the boundary conditions in the diffusion computation. The influence of temperature gradient along the membrane on the stress level was validated by experimental results. Low temperature gradient is required to decrease stress level.

Atmosphere variation rates were identified as a very dangerous step in term of stress development. Using a simplified analytical approach based on thermal stress analogy a "chemical shock" was defined that exhibits a linear dependence with oxygen partial pressure variation rate. These results show that the operating conditions control is a key point to ensure the reliability of the membrane.

Acknowledgment

The author wishes to thank Dr. G. Etchegoyen (CTTC, Limoges, France) for expansion tests and fruitful discussions.

References

1. Kharton, V. V., Yaramchenko, A. A., Patrakeev, M. V., Naumovich, E. N. and Marques, F. M. B., Thermal and Chemical induced expansion of $La_{0.3}Sr_{0.7}(Fe,Ga)O_{3-\delta}$ Ceramics. *J. Eur. Ceram. Soc.*, 2003, **23**, 1417–1426.
2. Krishnamurthy, R. and Sheldon, B. W., Stresses due to oxygen potential gradients in non-stoichiometric oxides. *Acta Materialia*, 2004, **52**(7), 1807–1822.
3. Atkinson, A. and Ramos, T. M. G. M., Chemically-induced stresses in ceramic oxygen ion-conducting membranes. *Solid State Ionics*, 2000, **129**(1–4), 259–269.
4. Fossdal, A., Menon, M., Waernhus, I., Wiik, K., Einarsrud, M.-A. and Grande, T., Crystal structure and thermal expansion of La1-xSrxFeO3-δ materials. *J. Am. Ceram. Soc.*, 2004, **87**(10), 1952–1958.
5. Hendriksen, P. V., Larsen, P. H., Mogensen, M., Poulsen, F. W. and Wiik, K., Prospects and problems of dense oxygen permeable membranes. *Catal. Today*, 2000, **56**, 283–295.
6. Kingery, W. D., Factor affecting thermal stress resistance of ceramic materials. *J. Am. Ceram. Soc.*, 1955, **38**(1), 3–15.
7. Hasselman, D. P., Unified theory of thermal shock fracture initiation and crack propagation in brittle ceramics. *J. Am. Ceram. Soc.*, 1969, **52**(11), 600–604.
8. Hasselman, D. P., Thermal stress resistance parameters for brittle refractory ceramics: a compendium. *Bull. Am. Ceram. Soc.*, 1970, **49**(12), 1033–1037.
9. Yakabe, H., Hishinuma, M. and Yasuda, I., Static and transient model analysis on expansion behavior of $LaCrO_3$ under oxygen potential gradient. *J. Electrochem. Soc.*, 2000, **150**, 35–45.
10. Yakabe, H. and Yasuda, I., Model analysis of the expansion behaviour of $LaCrO_3$ interconnector under solid oxide fuel cell operation. *J. Electrochem. Soc.*, 2003, **150**(1), A35–A45.
11. Adler, S. B., Chemical expansivity of electrochemical ceramics. *J. Am. Ceram. Soc.*, 2001, **84**(9), 2117–2119.
12. Kharton, V. V., Kovalevsky, A. V., Viskup, A. P., Jurado, J. R., Figueiredo, F. M., Naumovich, E. N. and Frade, J. R., Transport properties and thermal expansion of $Sr_{0.97}Ti_{1-x}Fe_xO_{3-\delta}$ ($x = 0.2$–0.8). *J. Solid State Chem.*, 2001, **156**, 437–444.
13. Zuev, A., Singheiser, L. and Hilpert, K., Defect structure and isothermal expansion of A-site and B-site substituted lanthanum chromites. *Solid State Ionics*, 2002, **147**, 1–11.
14. Etchegoyen, G., *Développement d'une membrane céramique conductrice mixte pour la production de gaz de synthèse*. Ph.D., in French, Univ. Limoges, France, 2005.
15. Blond, E., Schmitt, N., Hild, F., Poirier, J. and Blumenfeld, P., Modelling of high temperature asymmetric creep behaviour of ceramics. *J. Eur. Ceram. Soc.*, 2005, **25**(11), 1819–1827.
16. Miypshi, S. *et al.*, Lattice expansion upon reduction of perovskite-type $LaMnO_3$ with oxygen-deficit nonstoichiometry. *Solid State Ionics*, 2003, **161**, 209–217.
17. Miyoshi, S., Hong, J.-H. *et al.*, Lattice creation and annihilation of $LaMnO_{3+\delta}$ caused by nonstoichiometry change. *Solid State Ionics*, 2002, **154–155**, 257–263.
18. Abaqus, *Standard version 6.5*, *User's Manual*, 2004, ABAQUS, Inc.
19. *Fluent User Manual 6.2*, 2005, FLUENT, Inc.
20. Kharton, V. V., Kovalevsky, A. V. *et al.*, Oxygen transport in $Ce_{0.8}Gd_{0.2}O_{2-\delta}$-based composite membranes. *Solid State Ionics*, 2003, **160**, 247–258.
21. Hild, F. and Marquis, D., A statistical approach to the rupture of brittle materials. *Eur J. Mech. A/Solids*, 1992, **11**(6), 753–765.
22. Boley, B. A. and Weiner, J. H. In *Theory of Thermal Stress*. John Wiley and Sons, 1960.